Segment-constrained regression tree estimation of forest stand height from very high spatial resolution panchromatic imagery over a boreal environment

Brice Mora, Michael A. Wulder*, and Joanne C. White

Affiliation:

Canadian Forest Service, Pacific Forestry Centre, Natural Resources Canada, Victoria, BC, V8V 1M5, Canada

*Corresponding author:
Michael A. Wulder
Email: mike.wulder@nrcan.gc.ca; Phone: 250-363-6090; Fax: 250-363-0775

Pre-print of published version.

Reference:
Mora, B., M.A. Wulder, and J.C. White (2010). Segment-constrained regression tree estimation of forest stand height from very high spatial resolution panchromatic imagery over a boreal environment. Remote Sensing of Environment. Vol. 114, pp. 2474–2484.

DOI.
http://dx.doi.org/10.1016/j.rse.2010.05.022

Keywords: forest stand height, forest inventory, remote sensing, QuickBird, panchromatic, object-based, boreal, monitoring

Abstract

Mean stand height is an important parameter for forest volume and biomass estimation in support of monitoring and management activities. Information on mean stand height is typically obtained through the manual interpretation of aerial photography, often supplemented by the collection of field calibration data. In remote areas where forest management practices may not be spatially exhaustive or where it is difficult to acquire aerial photography, alternate approaches for estimating stand height are required. One approach is to use very high spatial resolution (VHSR) satellite imagery (pixels sided less than 1 m) as a surrogate for air photos. In this research we demonstrate an approach for modelling mean stand height at four sites in the Yukon Territory, Canada, from QuickBird panchromatic imagery. An object-based approach was used to generate homogenous segments from the imagery (analogous to manually delineated forest stands) and an algorithm was used to automatically delineate individual tree crowns within the segments. A regression tree was used to predict mean stand height from stand-level metrics generated from the image grey-levels and within-stand objects relating individual tree crown characteristics. Heights were manually interpreted from the QuickBird imagery and divided into separate sets of calibration and validation data. The effects of calibration data set size and the input metrics used on the regression tree results were also assessed. The approach resulted in a model with a significant R^2 of 0.53 and an RMSE of 2.84 m. In addition, 84.6% of the stand height estimates were within the acceptable error for photo interpreted heights, as specified by the forest inventory standards of British Columbia. Furthermore, residual errors from the model were smallest for the stands that had larger mean heights (i.e., >20m), which aids in reducing error in subsequent estimates of biomass or volume (since stands with larger trees contribute more to overall estimates of volume or biomass). Estimated and manually interpreted heights were reclassified into 5-metre height classes (a schema frequently used for forest analysis and modelling applications) and compared; classes corresponded in 54% of stands assessed, and all stands had an estimated height class that was within ± 1 class of their actual class. This study demonstrates the capacity of VHSR panchromatic imagery (in this case QuickBird) for generating useful estimates of mean stand heights in unmonitored, remote, or inaccessible forest areas.

Introduction

Tree height is a fundamental attribute for describing forest stands, as well as a critical parameter for indicating site quality (Véga and St-Onge, 2009; Wulder et al., 2009) and for estimating stand-level volume and biomass (Boudewyn et al., 2007; Falkowski et al., 2009). Forest inventory stand heights are typically interpreted from aerial photography (Avery and Burkhart, 2002: Hall, 2003), supplemented with field calibration data. Although the accuracy requirements for stand height estimates vary from one inventory to another, allowable error rates typically range between 10 and 15% (Rhody, 1965; Kayitakire et al., 2006). The accurate estimation of stand height from air photos is difficult in areas of dense forest where the ground is not visible (St. Onge et al., 2008). Alternative approaches for estimating stand height may be required in remote areas where forest management practices are not spatially exhaustive or where it is logistically difficult or not common practice to acquire aerial photography.

Canada's forests comprise 10% of global forest cover and occupy approximately 40% of Canada's landmass (Wulder et al., 2008a). Canada implements a multiphase, plot-based National Forest Inventory (NFI) for assessment and monitoring of forests. Approximately 1% of Canada's landmass is sampled in the NFI's first phase using a systematic network of 19,000 photo plots located on a 20 by 20 km sampling intensity grid, with each plot being 2 by 2 km in size. Within the photo plot, photo interpreters manually delineate forest stand boundaries from 1:20,000 scale aerial photography and then, using a combination of manual air photo interpretation and allometric models, determine a suite of required forest inventory attributes. In the second phase of the NFI, ground plots are established in a 10% random sample of photo plot locations (for a minimum of 50 ground plots per ecozone) (Gillis, 2001).

Several different remotely sensed data sources have been explored for forest height estimation. For example, C-band data from the Shuttle Radar Topography Mission (SRTM) and ancillary data have been used to estimate stand height in uniform stands of red and Austrian pine (Brown et al., 2010). However, radar data have limited capacity to facilitate stand delineation and estimation of other forest inventory attributes of interest (Kenyi et al., 2009), restricting the data's utility in a forest inventory context. Furthermore, tree density, tree structure, and ground slope can influence forest parameter estimation from radar data (Garesteir et al., 2009). The estimation of stand height with airborne lidar data has been the subject of extensive research (Lim et al., 2003) and lidar is now used in some operational forestry contexts. To date, the only spaceborne lidar system is the Geoscience Laser Altimeter System (GLAS). Some studies have investigated the use of GLAS for estimating canopy height, with varying levels of success (Lefsky et al., 2007; Duncanson et al., 2010). While airborne lidar data may represent the state-of-the-art for estimation of forest stand height (e.g., Naesset, 1997; Naesset and Økland, 2002), lidar can be an expensive monitoring option for extensive forest areas unless a sampling approach is adopted (Wulder and Seemann, 2003). Furthermore, airborne lidar faces certain acquisition constraints (Wulder et al., 2008), and lidar estimates of stand height may be impacted by complex terrain, steep slopes, and high canopy cover (Gatziolis et al., 2010). Andersen et al. (2006) also comment and remind that ground based measures have error typically with a range of 1 to 10 %, illuminating the difficulty in obtaining definitive accuracy for lidar – or in our case other measures – of tree height.

In Canada's northern region, financial and logistical constraints often preclude the acquisition of aerial photography. In response to these information gap, the NFI has used a Landsat-based land cover product, Earth Observation for Sustainable Development of Forests or EOSD (Wulder et al., 2008a), to provide a limited number of the required forest inventory attributes in areas where aerial photography has not been acquired (i.e., cover type, density, volume, and biomass) (Gillis et al., 2005). In addition, a framework has been developed that employs Very High Spatial Resolution (VHSR; < 1 m) remotely sensed imagery to support Canada's NFI programme, particularly in the north. It is envisioned that the use of VHSR will help to fill the data gap in the north, while at the same time, improving the consistency of attribute estimation between northern and southern photo plots. VHSR optical images provide spatial and spectral information that is similar to aerial photography and may be used for manual or semi-automated interpretation of forest inventory attributes (Wulder et al., 2008b). VHSR images are

being acquired by an increasing number of commercial sensors and have a high geometric fidelity. As identified in Falkowski et al. (2009), "incorporating VHSR satellite imagery into existing large-area, sample-based forest inventory frameworks may provide a means to increase overall inventory efficiency and precision."

Background

Several studies have demonstrated data and methods that have potential utility for estimating stand height using VHSR imagery. Hirata (2008) estimated stand density and stand volume in Japanese cedar (*Cryptomeria japonica*) and Japanese cypress (*Chamaecyparis obtusa)* stands using segmented QuickBird panchromatic imagery. Crown areas were calculated from the QuickBird imagery and these crown areas were used in an allometric relationship to estimate diameter-at-breast height (DBH). These DBH estimates were used in conjunction with height-diameter curves (determined by site quality) to estimate individual tree heights. From this information, volumes were calculated and compared to field-based estimates. Although the relationship between the derived and field-measured DBH values is reported (R=0.78, p<0.001), the reliability of the height estimates (e.g., RMSE) were not reported in this study.

Texture measures generated from 1-m IKONOS image grey levels were used to estimate stand top heights in even-aged Norway spruce (*Picea abies* (L.) Karst.) stands (Kayitakire et al., 2006). The authors found a strong relationship between estimated heights and field-measured heights (R^2=0.76; RMSE = 2.060; p<0.001). In a similar study, Chubey et al. (2006) used regression trees and a suite of 87 segment-level metrics from IKONOS-2 multispectral imagery to estimate stand height (among other variables) into one of four broad height classes. The accuracy of the height estimation, assessed using independent validation data, was found to be 49%.

Objectives

As indicated by these aforementioned studies, VHSR imagery can be used as a data source for forest inventory and assessment. The overall goal of this communication is to present a method for the automated estimation of stand height from VHSR QuickBird panchromatic imagery. It is envisioned that such a process would enable the consistent estimation of an important forest inventory attribute that is a critical input for a number of other modeled inventory attributes, such as volume and biomass. As such, the methods presented are intended to augment Canada's NFI VHSR framework (Falkowski et al., 2009). Using a regression tree approach, stand heights were estimated over four sample locations in the Yukon Territory, Canada. The accuracy of the estimated heights was assessed by a comparison to heights that were manually interpreted from the QuickBird imagery. The effects of varying calibration data set sizes and input parameters were also assessed. Although the process described is in support of Canada's NFI VHSR framework, the challenges identified are informative for stand-based forest inventories in general.

Methods

Study area

Four study sites located in the southern Yukon Territory were selected for possibility of access and related availability of QuickBird imagery (Figure 1). The size of the study sites ranged from 625 to 2400 ha (Table 1). All of the study sites were located in the Boreal Cordillera Ecozone (Ecological Stratification Working Group, 1995), which is

characterized by a climate ranging from cold and sub-humid to semi-arid. Mean annual temperatures range between 1°C to 5.5°C and mean annual precipitation ranges from less than 300 mm in valleys shadowed by coastal mountain ranges, to more than 1500 mm at higher elevations. The topography of the Boreal Cordillera Ecozone includes mountains and extensive plateaus, separated by wide valleys and lowlands. Glaciation, erosion, solifluction, and eolian and volcanic ash deposition have altered the original topography. Glacial drift, colluvium, and outcrops are the most common surface materials. Permafrost is widespread in the more northern areas of the ecozone. Depending on local conditions, tree species include white spruce (*Picea glauca*), black spruce (*Picea mariana*), alpine fir (*Abies lasiocarpa*), lodgepole pine (*Pinus contorta*), trembling aspen (*Populus tremuloides*), balsam poplar (*Populus balsamifera*), and white birch (*Betula papyrifera*). Forest disturbances in the Yukon Territory are primarily the result of wildfire, insects, and, to a lesser extent, forest harvesting.

<< Figure 1 about here >>

<< Table 1 about here >>

Data

QuickBird imagery

An 8 km by 8 km panchromatic (0.45–0.90 μm) QuickBird-2 image with a 0.61 m spatial resolution was acquired for each study site (see acquisition parameters listed in Table 1). As a result of the QuickBird sensor's variable cross-track and in-track viewing capability, the sensor has a temporal resolution that will vary according to the latitude of the end-user's area of interest and their tolerance for an off-nadir viewing angle. For instance, at 50° N latitude a revisit of 4 days (with up to 25° off-nadir) to 7 days (with up to 15° off-nadir), may be expected (DigitalGlobe, 2005). VHSR imagery such as QuickBird enables the detection of individual tree characteristics, which in turn can provide improved estimates of many forest inventory attributes (Wulder, 1998). Use of this data is not without challenges, owing to a lack of established methods for processing (Falkowski et al., 2009) and the complex interactions between sun-sensor-surface geometry and forest structural characteristics, particularly at more northerly latitudes (Wulder et al., 2008c).

Image pre-processing

The QuickBird images were delivered as 11-bit data, but were converted to 16-bit unsigned, resulting in a theoretical range of grey level values from 0 to 65536. The images were converted to top-of-atmosphere radiance as per Krause (2003) and were then orthorectified using a 15 m panchromatic Landsat-7 ETM+ orthoimage (Wulder et al., 2002a). All four sites were either on flat or gentle slopes (i.e. less than 5 %). The average RMSE for the orthorectification process was 5 m.

Image segmentation

Segmentation was used to delineate units with homogeneous forest conditions, analogous to forest stands delineated by manual interpretation (Wulder et al., 2008b). To avoid over-segmentation as a result of the high spatial resolution of the QuickBird image (Wang et al., 2004), the segmentation process was applied to a median filtered version of the original orthorectified QuickBird panchromatic band. The median filter applied to the images had a window size that was either 7-by-7 or 15-by-15 pixels. A median filter was chosen as it will likely produce more homogeneous image segments and may reduce the amount of convolution in the final segmented stand boundaries (Falkowski, 2009). The

segmentation was performed using Definiens Cognition Network Technology® (Baatz and Schäpe, 2000; Definiens Imaging, 2004). Through experimentation and development of an NFI protocol for segmentation (Henley et al., 2009; Falkowski et al., 2009), a set of initial segmentation parameters were determined: scale = 1200, color = 0.3, and compactness = 0.9 (Henley et al. 2009). The size of the filter window and the parameters were adjusted as required for each image in order to account for differences in land cover composition, as well as differences in vegetation structure and distribution. The final segments were reviewed manually to ensure quality (Wulder et al., 2008b).

Manual image interpretation

Photo interpreters certified by the British Columbia provincial government (Ministry of Forests and Range, 2009) manually interpreted and attributed (from the QuickBird image) each of the forested segments according to National Forest Inventory Photo Plot standards (Natural Resources Canada, 2004). Key attributes that were interpreted include species composition, age, crown closure, and height (Gillis et al., 2005). The manually interpreted heights were used for subsequent model calibration and validation.

Image classification

A land cover classification using four broad cover classes (forest, herb, exposed land, and water) was performed to determine the main land cover component within each segment, with the objective of excluding any non-forest segments from further analysis. The supervised fuzzy classifier in Definiens Cognition Network Technology® software was used to assign the cover type. This step was accomplished by manually establishing image grey level thresholds for each cover class. A subsequent iteration of the classifier was used to assign the forested class to either a coniferous or broadleaf subclass. Class definitions are those specified for the National Forest Inventory and Earth Observation for Sustainable Development (EOSD) of Forests (Wulder and Nelson, 2003).

Tree crown delineation

The spatial resolution of panchromatic QuickBird imagery (pixels sided 0.61 m) has been demonstrated to produce reliable tree crown delineation (Gougeon et al., 2003; Ozdemir, 2008), thereby enabling the inclusion of crown-based metrics into our model. The Individual Tree Crown (ITC) algorithm by Gougeon (1995) was chosen to delineate tree crowns within each of the forested segments and is available as an extension of the image processing software PCI Geomatica. The ITC algorithm has been proven effective over a range of image types and forest conditions (Gougeon et al., 2003; Leckie et al., 2003; Gougeon and Leckie, 2006). The ITC method requires an upper and lower grey level value threshold in order to determine whether a pixel represents a portion of a tree crown or represents the surrounding shadow or understorey. As recommended in Gougeon (2005), we applied a 3-by-3-pixel averaging filter to the panchromatic image prior to using the ITC algorithm.

Calculation of stand-level metrics

Stand-level measures of a panchromatic image's grey levels are known to be conditioned by canopy structural attributes such as crown closure, tree height, and stand type (Parker et al., 1995; Asner et al., 2003). Furthermore, local topography and image acquisition parameters also influence image grey levels (Itten et al., 1992; Leckie et al., 1992; Wulder et al., 2008c). In this study, stand-level summary measures of image grey levels were used as inputs for regression trees in the estimation of stand height. The following statistics were calculated for the image grey levels in each forested segment: majority,

minority, median, mean, standard deviation, range, and the number of unique values of all pixels in the segment (variety). Segment grey-level values were also examined to remove any outliers from subsequent analysis (i.e., segments containing grey-level values that were 3 or more standard deviations from the segment mean grey-level).

From the crowns delineated with ITC, segment-level estimates of crown closure, mean crown size, and the 25^{th}, 50^{th}, and 75^{th} percentiles of crown size distribution were generated. Forested segments with a crown closure less than 10% were considered non-forest (Wulder and Nelson, 2003; Boudewyn et al., 2007) and were excluded from further analysis.

Regression tree development

A regression tree approach was selected for this analysis because it is non-parametric, it can accommodate both discrete (i.e., stand type) and continuous variables, and it can account for non-linear relationships between model inputs and output targets. Moreover regression trees tend to be robust to errors in both the independent and dependent variables (Breiman et al., 1998). Regression trees function by recursively partitioning a dataset into increasingly homogenous subsets. Regression trees were implemented using the *R* software (*R* Development Core Team, 2005) and the package *tree* (Ripley, 2009).

Model calibration

Each of the stand segments used as inputs to the regression tree were characterized by the thirteen aforementioned stand-level statistics. The data set, consisting of 189 forested segments, was randomly split into separate calibration (70% of segments) and validation (30% of segments) sets. In order to ensure a non-biased evaluation of the results, we used a Multi Response Permutation Procedure (Mielke and Berry, 2001) to evaluate the degree to which the calibration and validation data were representative of the entire data set. This non-parametric method tests the hypothesis of no difference between two or more data sets for a range of parameters (i.e., the stand-level metrics used as inputs to the regression tree).

Selection of input metrics

Since some of the stand-level metrics involve significant computational overhead to produce (i.e., crown-based metrics), a Hill-Smith test (Hill and Smith, 1976) was applied to the entire data set to identify those input metrics with the strongest positive or negative correlations to the manually interpreted stand heights. The objective of this test was to identify an optimal set of inputs to the regression tree, thereby reducing the number of input metrics required and resulting in a more efficient protocol for modeling stand height from the QuickBird-based metrics. The Hill-Smith test is multivariate and measures correlations between both categorical (e.g., stand type) and numerical variables (e.g., mean crown size). The regression trees were run twice: once using all of the input metrics, and once using only the optimal inputs. The resulting height estimates were assessed using the same set of validation data, and then compared.

Regression tree parameters

For each regression tree, a *K*-fold cross-validation ($K = 10$) was processed, followed by a tree pruning stage applied according to best practices regarding tree size (McLachlan et al., 2004). We averaged the estimated mean stand heights from each iteration to produce the final mean stand height values.

Optimizing the size of the calibration data set

Manual interpretation of imagery for forest inventory is time consuming, costly, and inconsistent for some attributes (Wayman et al., 2001; McRoberts et al., 2002). Consequently, as part of this study, we wanted to assess the impact of reducing the number of manually interpreted stands required for calibration of the regression tree model. We measured the impact of the calibration sample size on stand height estimation accuracy by varying the size of the calibration dataset, which ranged from 10% to 100% of the forested segments, in 10% increments. For each iteration, the segments used for calibration were selected at random and the regression tree was applied; this process was repeated 100 times for each calibration sample size.

Model validation

Manually interpreted heights were used for validation. The coefficient of determination (R^2), *p*-value, and root mean square error (RMSE) were calculated to characterize the quality of the model and the results. Similarly, scatterplots of modeled versus manually interpreted heights, and scatterplots of residuals were generated and examined. A Welch test (Welch, 1947) was used to compare the photo interpreted and the modeled stand heights (for all calibration data set sizes). This statistical test was selected because the distributions for mean stand heights were normal and variances for photo interpreted and modeled heights were significantly different.

Many applications that use stand height to model other attributes (e.g., timber supply and carbon budget modelling) will group this metric into 5 m height classes prior to analysis (Trofymow et al., 2008, Wulder et al., 2009). Therefore to further assess the reliability of our height estimates for this purpose, we categorized our mean stand heights for the validation sample into the NFI 5-metre height classes (using the results from the regression tree model generated from the 30% sample of calibration data). We similarly categorized the manually interpreted heights into the same classification hierarchy and compared these to our estimated height classes.

Results and Discussion

Image segmentation and classification

The segmentation parameters we used resulted in segments that complied with the NFI's requirement for a minimum polygon size of 2 ha for forested polygons (Natural Resources Canada, 2004) (Figure 2, a). A total of 426 segments were generated, of which 68% were forested with a mean segment size of 4.9 ha (Table 2). Approximately 76% of the forested segments were coniferous and 24% were broadleaf. Overall, the coniferous segments had a larger mean segment size at 5.14 ha, compared to 4.18 ha for the broadleaf segments.

<<Table 2 about here>>

<< Figure 2 about here >>

Manual image interpretation and tree crown delineation

All of the forested segments at all four sites (N = 291) were manually interpreted according to NFI standards (Natural Resources Canada, 2004). Individual tree crowns in the forested segments, as delineated by the ITC program, had a mean size of 8.2 m^2 (Table 3, Figure 2,b). Given that the proportion of stands dominated by coniferous species (77%) is greater than the proportion of stands dominated by broadleaf species

(23%), the mean crown size for coniferous dominated stands is closer to the mean crown size for the full data set. The distributions of crown sizes for both broadleaf and coniferous stands were normal (Jarque-Bera test, with *p*-values of 0.36 and 0.17 for broadleaf and coniferous respectively), and a Fisher test indicated that the crown size variances for each stand type were not equal (*p*-value = $1.15.e^{-10}$). Consequently, we conducted a Welch test to compare the mean crown size for each stand type, and found that there was a significant difference (*p*-value = $2.71.e^{-7}$) between the mean crown size in broadleaf and coniferous stands.

<<Table 3 about here>>

There is a known relationship between crown diameter and tree height (Peper et al., 2001; Avsar, 2004; Morsdorf et al., 2004), and between crown diameter and tree bole diameter (diameter at breast height (DBH)) (Zhang, 1997; Bechtold 2004, Hemery et al. 2005). Hirata (2008) used an understanding of these relationships to estimate both DBH and height from individual tree crowns delineated from QuickBird panchromatic imagery. Likewise, by including tree crown parameters as inputs to our regression tree, we sought to similarly exploit these known relationships.

Calculation of stand-level metrics

Stand-level metrics were calculated and used to screen for outliers. Table 4 summarizes the metric statistics over the entire set of delineated stands. Of the 291 forested segments identified, 37 segments were excluded from further analysis because they contained grey level outliers (i.e., grey levels that were 3 or more standard deviations from the segment mean grey level). As with any regression-based approach, the detection and removal of outliers is an important prerequisite for establishing a robust model. An additional 65 segments with less than 10% crown closure were also excluded from further analysis as these segments would be considered non-forest according to NFI specifications (Natural Resources Canada, 2004). In total, 189 forested stands remained for subsequent analysis and height estimation. The segmentation process produced forested stands with crown closure values that had a relatively limited range (i.e., between 40 and 55%), mirroring the photo interpreted crown closure conditions present over the study area.

<<Table 4 about here>>

Regression tree estimation of stand height

Model calibration

The 189 forested segments were partitioned into separate calibration (N = 132) and validation (N =57) data sets and the MRPP test indicated a chance-corrected within-group agreement of $-1.8*10^{-3}$ and a *p*-value of 0.65, demonstrating that there were no significant differences between the calibration and validation data sets (considering all of the stand-level metrics).

Selection of input metrics

The results of the Hill-Smith test indicated that the 25^{th}, 50^{th}, and 75^{th} percentiles of the segment-level crown size distribution, as well as the mean segment crown size, were the variables with the strongest correlation to the manually interpreted mean stand heights. Figure 3 illustrates the correlations between variables in the space created by the two first principal components (72% of the variance is explained in this space).

<< Figure 3 about here >>

Two different scenarios were explored for the automated estimation of stand height with the regression tree. The first scenario used all thirteen stand-level metrics as inputs, while the second scenario used only those four inputs that were most strongly correlated with the manually interpreted stand heights. The independent set of validation data was used to assess the performance of the regression tree models. The RMSE and R^2 values (with the associated *p*-value) for both scenarios are summarized in Table 5. Higher R^2 values and lower RMSE values were obtained with the full set of input parameters, regardless of the size of the calibration data set. This result suggests that although the identified optimal subset of input metrics may be more strongly correlated with the manually interpreted stand heights, this subset is insufficient for generating robust estimates of stand height.

<< Table 5 about here >>

The main stand-level metrics used in the regression tree, by frequency of occurrence and in decreasing order were: majority, standard deviation, minority, range, and mean grey level, as well as mean crown size. These results confirm the need to use both segment-based grey-level metrics as well as crown-based information to accurately model mean stand height. Multiple selection of a given metric in the same tree occurred in 15% of cases, with all trees having between two and four metrics, regardless of the regression tree structure. Similar to the range of photo interpreted crown closure values, the segmentation process produced forest stands that had a limited range of crown closure values (i.e., between 40 and 55%); as a result, there was little correlation between crown closure and interpreted stand height (Figure 3). Crown closure was not selected in any of the regression tree models.

Stand type (coniferous versus broadleaf) was only selected in 0.5% of regression trees, indicating that stand type does not play a significant role in tree height estimation. We performed a Student's *t*-test on the mean residual distributions from both stand types for the 30% calibration sample size (all 13 input metrics) to further explore the effect of stand type on the estimation of mean stand height. The t-test was chosen as residual distributions were found to be normal (χ^2 of 0.1 and 0.3) according to the Jarque-Bera test (Jarque and Bera, 1987) and as variances were found to be equal (*p*-value of 0.70 for the Fisher test). No significant difference between residuals was found (*p*-value of 0.15). This result confirms that in this environment, the stand type had no significant impact on tree height estimation. As a result, we would not recommend that the calibration data be stratified by stand type, but rather that the calibration data is selected to represent the distribution of mean stand heights in the study area.

Optimizing the size of the calibration data set

At the outset of our study, we had set aside 132 stands for model calibration. We then assessed the impact that the size of the calibration data set had on the estimates of mean stand height that were generated from the regression tree. Initially, we used 10% of the calibration data to train the model, increasing the sample size in 10% increments. Note that the small size of the 10% sample resulted in the systematic generation of single nodes in the regression tree and as a result, the R^2 value could not be calculated as the standard deviation of the estimated height distribution was null. The model R^2 values decreased as the size of the calibration data set increased (Table 5). In the case where all metrics were used as input, regression trees using 20, 30, or 40% of the calibration data were significant ($p < 0.01$); using only the optimal metrics as input, all of the regression models were significant ($p < 0.01$) (Table 5). Height estimates generated from the 30%

sample of calibration data (all input metrics) had an R^2 of 0.5 and an RMSE of 2.71 m, compared to an R^2 of 0.26 and an RMSE of 3.10 m that resulted from using 100% of the calibration data. It is generally understood that the accuracy of decision tree models tends to increase with increasing calibration sample size until a certain threshold is reached, at which point accuracy will begin to decrease; however, this threshold is ambiguous and dependent on the particular application and the source data used (Pal and Mather, 2003). The RMSEs of our models do not follow such a clear trend; however, since the approach we present for estimating mean stand height from VHSR requires some minimal amount of calibration data, there is a trade-off to be made between the amount of calibration data acquired through manual interpretation and the robustness of the model estimates. Furthermore, it is important to note that the manually interpreted heights that were used as calibration data are not without error. Error rates for the manual interpretation of forest inventory stand heights are typically reported to be between 10 and 15% (e.g., Rhody, 1965; Kayitakire et al. 2006). Such errors in the calibration data will have an impact on model estimates.

Model validation

The comparison of the photo interpreted and the estimated heights with the Welch test indicated that the manually interpreted and modeled height distributions were not significantly different ($p > 0.05$) (Table 6). Figure 4 illustrates the manually interpreted mean stand heights versus the estimated heights for the 30% calibration sample size case. Figures 5 and 6 are plots of the manually interpreted heights against the absolute residuals and residual values for the regression tree generated from the 30% calibration sample size, respectively. The lowest residuals were for stands with mean heights ranging from 20 to 23 m (Figure 5). As indicated in Figure 5 and 6, the residuals were not randomly distributed: the regression tree overestimated height for stands with a manually interpreted small mean stand height and underestimated height for stands with a manually interpreted large mean stand height. Although the largest residuals were associated with the smaller trees, this error would have less impact on the calculation of volume and biomass, since the larger trees contribute more to these estimates (Wulder et al. 2002b).

<< Table 6 about here >>

<< Figure 4 about here >>

<< Figure 5 about here >>

<< Figure 6 about here >>

A comparison of the height classes between the estimated and manually interpreted data indicated that height class assignments agreed for 54% of the segments used for validation. Furthermore, all of the misclassifications were within ± one adjacent height class. This result compares to the 49% accuracy of Chubey et al. (2006), in which broad height classes were used to compare manually interpreted heights to height estimates generated from segmented IKONOS imagery, supporting this previous work and buttressing our current findings.

Although the NFI does not have a specific quality control standard for the photo interpretation of height, many provincial forest management agencies in Canada do have such standards. For example, in British Columbia, photo interpreted leading species height must be within ± 3 metres or 15% (whichever is greater) of the actual height value (Ministry of Forests and Range, 2009); 84.6% of our mean stand height estimates were within this level of acceptable error. In the Yukon Territory, where our study sites were

located, quality control standards for photo interpretation of height specify that estimates for leading species height must be within ± 1 m of actual height (Department of Energy, Mines, and Resources, 2006). However, it is not common practice to assess the agreement of forest inventory attribution to the standards (Thompson et al. 2007), with the nature of the agreement complicated by differences in ground measurement techniques and scale to what can be discerned from above in the imagery. Standards are used to guide the quality and rigour of the interpretation process and do not necessarily indicate the accuracy of the resultant map products. Variation in sun-surface-sensor geometry may also limit the agreement between manually interpreted and modeled mean stand heights. To enable a reasonable opportunity for capture of imagery, we have specified an off-nadir view angle of 0-15 degrees for product purchase (and a consistent range of image conditions). The true nadir revisit cycle of high spatial resolution sensors varies (see Wulder et al., 2008c; Falkowski et al. 2009), with too limited a product specification, combined with cloud cover, limiting acquisition opportunities and creating operational risk. The design of our regression trees assumes that stand height has the greatest influence on image grey levels; such an assumption may underestimate the influence of different image acquisition parameters (Table 1) on the variability of image grey levels (Wulder et al., 2008c) and on the subsequent delineation of individual tree crowns. Furthermore, the manually interpreted heights used for calibration and validation of the model are themselves not without bias (Eid et al., 2005). While the use of *in situ* measurements would certainly strengthen the methodology we have presented, a model that is reliant on ground measurements would not be practical given Canada's vast northern forest area.

Conclusion

In this study, we modeled mean stand height using metrics generated from panchromatic QuickBird images as inputs to a regression tree. We compared these estimates to mean stand heights that were manually interpreted from the same QuickBird image. The study showed that low RMSEs can be obtained with smaller amounts of calibration data. This suggests that there may be efficiencies that are possible in the implementation of such an approach to augment existing NFI protocols. The results of this study also demonstrated that both stand-level metrics and information on tree crown sizes are necessary to obtain robust estimates of mean stand height. Furthermore, crown closure was not found to be informative to the regression tree models and stand type (e.g., coniferous, broadleaf) had no influence on the performance of the regression models. Statistically, the best model had an R^2 of 0.53 and an RMSE of 2.84 m, and 84.6% of our mean stand height estimates were within the level of acceptable error specified in the British Columbia forest inventory standards. Estimated and manually interpreted heights were reclassified into 5 m height classes and compared; classes corresponded for 54% of stands assessed, and *all* stands had an estimated height class within ± 1 class of their actual class. This study demonstrates the potential of VHSR panchromatic imagery for acquiring estimates of mean stand heights in remote or inaccessible forest areas. Given the difficulty in using optical remotely sensed data to relate a vertically distributed attribute – stand height – the results are positive and encouraging. Future work may focus first on using ground-based data for the calibration and validation of the method, and secondly on integrating

additional data sources and/or metrics into the regression tree models to further improve the estimation of mean stand height.

Acknowledgements

This research was undertaken as part of the "EcoMonitor: Northern Ecosystem Climate Change Monitoring" project jointly funded by the Canadian Space Agency (CSA) Government Related Initiatives Program (GRIP) and the Canadian Forest Service (CFS) of Natural Resources Canada. Dr. François Gougeon, of the CFS, is thanked for access and assistance with the ITC software used in this study.

References

Andersen, H.E., Reutebuch, S.E., McGaughey, R.J. 2006. A rigorous assessment of tree height measurements obtained using airborne lidar and conventional field methods. *Canadian Journal of Remote Sensing*, Vol. 32. pp. 355-366.

Asner, G.P., Scurlock, J.M.O., and Hicke, J.A. 2003. Global synthesis of leaf area index observations: implications for ecological and remote sensing studies. *Global Ecology and Biogeography,* Vol. 12, No. 3, pp. 191–205.

Avery, T.E., and Burkhart, H.E. 2002. *Forest Measurements*, Fifth Edition. McGraw Hill, Madison WI.

Avsar, M.D. 2004. The relationships between diameter at breast height, tree height and crown diameter in Calabrian Pines (*Pinus brutia* Ten.) of Baskonus Mountain, Kahramanmaras, Turkey. *Journal of Biological Sciences,* Vol. 4, No. 4, pp. 437–440.

Baatz, M., and Schäpe, M. 2000. Multiresolution segmentation: an optimization approach for high quality multi-scale image segmentation. *Proceedings of Angewandte Geographische Informationsverarbeitung XII*. Edited by Strobl, J., Blaschke, T.,Griesebner, G. Beiträge zum AGIT Symposium, Salzburg 2000, pp. 12–23.

Bechtold, W.A. 2004. Largest-crown-width prediction models for 53 species in the western United States. *Western Journal of Applied Forestry*, Vol. 19, No. 4, pp. 245–251.

Boudewyn, P., Song, X., Magnussen, S., and Gillis, M.D. 2007. *Model-based, volume-to-biomass conversion for forested and vegetated land in Canada*. Canadian Forest Service, Pacific Forestry Centre, Victoria, British Columbia. BC-X-411.

Breiman, L., Friedman, J.H, Olshen, R.A, and Stone, C.J. 1998. *Classification and Regression trees.* Chapman and Hall/CRC, Boca Raton, USA.

Chubey, M.S., Franklin, S.E., and Wulder, M.A. 2006. Object-based analysis of IKONOS-2 imagery for extraction of forest inventory parameters. *Photogrammetric Engineering and Remote Sensing*, Vol. 72, No. 4, pp. 383–394.

Definiens Imaging. 2004. *eCognition Elements: User Guide 4*. München, Germany.

Department of Energy, Mines, and Resources. 2006. *Yukon Vegetation Inventory Manual, Version 2.1*. Forest Management Branch, Whitehorse, Yukon.

DigitalGlobe. 2005. QuickBird Imagery Products FAQ. Satellite Imaging Corporation, Houston, Texas, USA. Available from: www.satimagingcorp.com/satellite.../quickbird_imagery_products.pdf [cited January 12, 2010].

Duncanson, L.I., Niemann, K.O., Wulder, M.A. 2010. Estimating forest canopy height and terrain relief from GLAS waveform metrics. *Remote Sensing of Environment*, Vol. 114, pp. 138–154.

Ecological Stratification Working Group. 1995. *A National Ecological Framework for Canada.* Agriculture and Agri-Food Canada, Research Branch. Ottawa. Available from: http://sis.agr.gc.ca/cansis/nsdb/ecostrat/intro.html [cited December 21, 2009].

Eid, T., Gobakken, T., and Næsset, E. 2005. Comparing stand inventories for large areas based on photo-interpretation and laser scanning by means of cost-plus-loss analyses. *Scandinavian Journal of Forest Research*, Vol. 19, No. 6, pp. 512–523.

Falkowski, M.J., Wulder, M.A., White, J.C., and Gillis, M.D. 2009. Supporting large-area, sample-based forest inventories with very high spatial resolution satellite imagery. *Progress in Physical Geography*. Vol. 33, No. 3, pp. 403–423.

Garestier, F., Dubois-Fernandez, P.C., Guyon, D., and Le Toan, T. 2009. Forest biophysical parameter estimation using L- and P-band polarimetric SAR data. *IEEE Transactions on Geoscience and Remote Sensing*, Vol. 47, pp. 3379–3388.

Gatziolis, D., Fried, J.S., Monleon, V.S. 2009. Challenges to estimating tree height via LiDAR in closed-canopy forests: a parable from western Oregon. *Forest Science*, Vol. 56, pp. 139–155.

Gillis, M.D. 2001. Canada's National Forest Inventory (Responding to current information needs). *Environmental Monitoring and Assessment*, Vol. 67, No. 1–2, pp. 121–129.

Gillis, M.D., Omule, A.Y., and Brierley, T. 2005. Monitoring Canada's forests: The National Forest Inventory. *The Forestry Chronicle*, Vol. 81, No. 2, pp. 214–221.

Gougeon, F.A. 1995. A crown-following approach to the automatic delineation of individual tree crowns in high spatial resolution aerial images. *Canadian Journal of Remote Sensing*, Vol. 21, No. 3, pp. 274–284.

Gougeon, F.A., Cormier, R., Labrecque, P., Cole, B., Pitt, D., and Leckie, D. 2003. Individual Tree Crown (ITC) delineation on Ikonos and QuickBird imagery: the Cockburn Island Study. In *Proceedings of the 25th Canadian Symposium on Remote Sensing*, 14–16 October 2003, Montréal, Québec.

Gougeon, F.A. and Leckie, D.G. 2006. The individual tree crown approach applied to IKONOS images of a coniferous plantation area. *Photogrammetric Engineering and Remote Sensing*, Vol. 72, No.11, pp. 1287–1297.

Hall, R.J. 2003. The roles of aerial photographs in forestry remote sensing image analysis. In *Remote Sensing of Forest Environments, Concepts and Case Studies*. Edited by M. A. Wulder and S.E. Franklin. Kluwer Academic Publishers, Boston. pp. 47–76.

Hemery, G.E., Savill, P.S., and Pryor, S.N. 2005. Applications of the crown diameter–stem diameter relationship for different species of broadleaved trees. *Forest Ecology and Management*, Vol. 215, No. 1–3, pp. 285–294.

Henley, M.J., Wulder, M.A., Falkowski, M.J. 2009. *EcoMonitor Segmentation Methodology, Version 2.0*. Canadian Forest Service, Pacific Forestry Centre, Victoria, British Columbia.

Hill, M.O., and Smith, A.J.E. 1976. Principal component analysis of taxonomic data with multi-state discrete characters. *Taxon,* Vol. 25, No. 2–3, pp. 249–255.

Hirata, Y. 2008. Estimation of stand attributes in *Cryptomeria japonica* and *Chamaecyparis obtusa* stands using QuickBird panchromatic data. *Journal of Forest Research*, Vol. 13, No. 3, pp. 147–154.

Itten, K.I., Meyer, P., Kellenberger, T., Leu, R., Sandmeier, S., Bitter, P., and Seidel, K. 1992. Assessment and correction of the impact of topography and atmosphere on remote sensing forest mapping of alpine regions. In *Proceedings of the European ISY Conference*, 30 March–4 April, 1992. Munich, Germany, ESA Publication Division, ESTEC, Noordwijk, The Netherlands. pp. 1369–1372.

Jarque, C.M., and Bera, A.K. 1987. A test for normality of observations and regression residuals. *International Statistical Review*, Vol. 55, No. 2, pp.163–172.

Kayitakire, F., Hamel, C., and Defourny, P. 2006. Retrieving forest structure variables based on image texture analysis and IKONOS-2 imagery. *Remote Sensing of Environment*, Vol. 102, No. 3–4, pp. 390–401.

Kenyi, L.W., Dubayah, R., Hofton, M., Schardt, M. 2010. Comparative analysis of SRTM-NED vegetation canopy height to LIDAR-derived vegetation canopy metrics. *International Journal of Remote Sensing*, Vol. 30, pp. 2797–2811.

Krause, K. 2003. *Radiance Conversion of QuickBird Data - Technical note*. Digital Globe, Longmont, CO.

Leckie, D.G., Gougeon, F.A, Walsworth, N., and Paradine, D. 2003. Stand delineation and composition estimation using semi-automated individual tree crown analysis. *Remote Sensing of Environment*, Vol. 85, No. 3, pp. 355–369.

Leckie, D.G., Yuan, X., Ostaff, D.P., Piene, H., and MacLean, D.A. 1992. Analysis of high spatial resolution multispectral MEIS imagery for spruce budworm damage assessment on a single tree basis. *Remote Sensing of Environment*, Vol. 40, No. 2, pp. 125–136.

Lefsky, M.A., Keller, M., Pang, Y., de Camargo, P.B., Hunter, M.O. 2007. Revised method for forest canopy height estimation from Geoscience Laser Altimeter System waveforms. *Journal of Applied Remote Sensing*, Vol. 1, 013537, pp. 1–18.

Lim, K.; Treitz, P.; Wulder, M.; St-Onge, B., and Flood, M. 2003. Lidar remote sensing of forest structure. Progress in Physical Geography. Vol. 27(1), pp. 88–106.

McLachlan, G.J., Do, K.A., and Ambroise, C. 2004. *Analyzing microarray gene expression data*. John Wiley and Sons, Hoboken, New Jersey.

McRoberts, R.E., Wendt, D.G, Nelson, M.D., and Hansen, M.H. 2002. Using a land cover classification based on satellite imagery to improve the precision of forest inventory area estimates. *Remote Sensing of Environment*, Vol. 81, No. 1, pp. 36–44.

Mielke, P.W., Jr., and Berry. K.J. 2001. *Permutation methods: A distance function approach*. Springer-Verlag, New York.

Ministry of Forests and Range, 2009. *Vegetation Resources Inventory: Photo Interpretation Quality Assurance Procedures and Standards, Version 3.2*. Forest Analysis and Inventory Branch, Victoria, British Columbia. Available online: http://www.for.gov.bc.ca/hts/vri/standards/index.html#photo

Morsdorf, F., Meiera, E., Kötza, B., Ittena, K.I., Dobbertine, M., and Allgöwerb, B. 2004. LIDAR-based geometric reconstruction of boreal type forest stands at single tree level for forest and wildland fire management. *Remote Sensing of Environment,* Vol. 92, No. 3, pp. 353–362.

Næsset, E. 1997. Determination of mean tree height of forest stands using airborne laser scanner data. *ISPRS Journal of Photogrammetry and Remote Sensing,* Vol. 52, pp. 49–56.

Næsset, E., Økland, T. 2002. Estimating tree height and tree crown properties using airborne scanning laser in a boreal nature reserve. *Remote Sensing of Environment*, Vol. 79, pp. 105–115.

Natural Resources Canada. 2004. *Canada's National Forest Inventory: Photo Plot Guidelines, Version 1.1. Internal Design Document*. Canadian Forest Service, Pacific Forestry Centre, Victoria, British Columbia.

Nelson, R., Boudreau, J., Gregoire, T. G., Margolis, H., Næsset, E., Gobakken, T., and Ståhl, G. 2009. Estimating Quebec Provincial Forest Resources Using ICESat/GLAS. Canadian Journal of Forest Research. Vol. 39, pp. 862–881.

Ozdemir, I. 2008. Estimating stem volume by tree crown area and tree shadow area extracted from pan-sharpened Quickbird imagery in open Crimean juniper forests, *International Journal of Remote Sensing*, Vol. 29, No. 19, pp. 5643–5655.

Pal, M., and Mather P.M. 2003. An assessment of the effectiveness of decision tree methods for land cover classification. *Remote Sensing of Environment,* Vol. 86, No. 4, pp. 554–565.

Parker, G.G., Lowman, M., and Nadkarni, N. 1995. Structure and microclimate of forest canopies. In *Forest Canopies: A review of research on a biological frontier*. Edited by M.D. Lowman and N.M. Nadkarni. Academic Press, San Diego. pp. 73–106.

Peper, P.J, McPherson, G.E., and Mori, S.M. 2001. Equations for predicting diameter, height, crown width, and leaf area of San Joaquin Valley street trees, *Journal of Arboriculture,* Vol. 27, No. 6, pp. 306–317.

R Development Core Team. 2005. R: a language and environment for statistical computing. R Foundation for Statistical Computing, Vienna, Austria, www.R-project.org.

Rhody, B.F. 1965. Photointerpretation and mapping for forestry purposes. *Unasylva*, [online], Vol. 19, No. 2. Available from: http://www.fao.org/DOCREP/24755E/24755e00.htm#Contents [cited December 21, 2009].

Ripley, B. 2009. tree: Classification and regression trees. R package version 1.0-27. http://CRAN.R-project.org/package=tree

St-Onge, B., Véga, C., Fournier, R. A., and Hu, Y. 2008. Mapping canopy height using a combination of digital stereo-photogrammetry and lidar, *International Journal of Remote Sensing*, Vol. 29, No. 11, pp. 3343–3364.

Thompson, I. D., Maher, S. C., Rouillard, D. P., Fryxell, J. M., and Baker, J. A. 2007. Accuracy of forest inventory mapping: Some implications for boreal forest management. *Forest Ecology and Management*.; Vol. 252, pp. 208–221.

Trofymow, J.A., Stinson, G., and Kurz, W.A. 2008. Derivation of a spatially explicit 86-year retrospective carbon budget for a landscape undergoing conversion from old-growth to managed forests on Vancouver Island, BC. *Forest Ecology and Management*, Vol. 256, No. 10, pp. 1677–1691.

Véga, C. and St-Onge, B. 2009. Mapping site index and age by linking a time series of canopy height models with growth curves. *Forest Ecology and Management*, Vol. 257**,** No. 3, pp. 951–959.

Wang, L., Sousa, W.P., and Gong, P. 2004. Integration of object-based and pixel-based classification for mapping mangroves with IKONOS imagery. *International Journal of Remote Sensing*, Vol.25, No.24, pp.5655–5668.

Wayman, J.P., Wynne, R.H., Scrivani, J.A., and Reams, G.R. 2001. Landsat TM-based forest area estimation using iterative guided spectral class rejection, *Photogrammetric Engineering and Remote Sensing*, Vol. 67**,** No. 10, pp. 1155–1165.

Welch, B. L. 1947. The generalization of "Student's" problem when several different population variances are involved. Biometrika, Vol. 34 (1–2), pp. 28–35.

Wulder, M.A. 1998. Optical remote sensing techniques for the assessment of forest inventory and biophysical parameters. *Progress in Physical Geography*, Vol. 22, No. 4, pp. 449–76.

Wulder, M.A., Loubier, E., and Richardson, D. 2002a. Landsat-7 ETM+ orthoimage coverage of Canada. *Canadian Journal of Remote Sensing*, Vol. 28, No. 5, pp. 667–671.

Wulder, M.A., Niemann, K. O. and Goodenough, D.G. 2002b. Error reduction methods for local maximum filtering, Canadian Journal of Remote Sensing, Vol. 28, No. 5. pp. 621–628.

Wulder, M.A., and Nelson, T. 2003. EOSD *Land Cover Classification Legend Report, Version 2*. Canadian Forest Service, Pacific Forestry Centre, Victoria, British Columbia. Available from: http://www.pfc.forestry.ca/EOSD/cover/EOSD_legend_report-v2.pdf [cited December 21, 2009].

Wulder, M.A., Seemann, D. 2003. Forest inventory height update through the integration of LiDAR data with segmented Landsat imagery. *Canadian Journal of Remote Sensing*, Vol. 29, pp. 536–543.

Wulder, M.A., White, J.C., Cranny, M., Hall, R.J., Luther, J.E., Beaudoin, A., Goodenough, D.G., and Dechka, J.A. 2008a. Monitoring Canada's Forests. Part 1: Completion of the EOSD Land Cover Project. *Canadian Journal of Remote Sensing*, Vol. 34, No. 6, pp. 549–562.

Wulder, M.A., White, J.C., Hay, G.J., and Castilla, G. 2008b. Towards automated segmentation of forest inventory polygons on high spatial resolution satellite imagery. *The Forestry Chronicle*, Vol. 84, No. 2, pp. 221–230.

Wulder, M.A., Ortlepp, S.M., White, J.C., and Coops, N.C. 2008c. Impact of sun-surface sensor geometry upon multitemporal high spatial resolution satellite imagery. *Canadian Journal of Remote Sensing*, Vol. 34, No.5, pp. 455–461.

Wulder, M.A., White, J.C., Stinson, G., Hilker, T., Kurz, W.A, Coops, N.C., St-Onge, B., and Trofymow, J.A. 2009. Implications of differing input data sources and approaches upon forest carbon stock estimation. *Environmental Monitoring and Assessment*, doi: 10.1007/s10661-009-1022-6.

Wulder, M.A., Bater, C.W., Coops, N.C., Hilker, T., White, J.C. 2008. The role of LiDAR in sustainable forest management. *The Forestry Chronicle*, Vol. 84, pp.807–826.

Zhang, L. 1997. Cross-validation of non-linear growth functions for modelling tree height-diameter relationships. *Annals of Botany,* Vol. 79, No. 3, pp. 251–257.

List of Tables

List of Figures

Table 1. QuickBird image acquisition parameters.

	Size (ha)	Plot center UTM Zone 9N		Acquisition date	Solar azimuth (degrees)	Solar elevation (degrees)	Satellite azimuth (degrees)	Satellite elevation (degrees)	Off-nadir view angle (degrees)	In-track view angle (degrees)	Cross-track view angle (degrees)
		Easting (m)	Northing (m)								
Site 1	625	45116	7133046	2007-08-28	176.6	35.7	197.3	77.3	11.6	-11.7	-0.2
Site 2	2400	118968	7030079	2007-08-18	174.5	39.9	175.8	84.1	5.3	-5.0	1.8
Site 3	625	130603	6866945	2006-06-12	171.8	51.4	57.2	78.5	10.9	8.1	7.3
Site 4	1375	508030	6661737	2007-06-08	172.9	52.8	173.1	88.3	1.3	-1.3	0.4

Table 2. Number and size of image segments, by site.

	Total number of segments	Total number of forested segments	Mean forested segment size (ha)	Total number of coniferous segments	Mean coniferous segment size (ha)	Total number of broadleaf segments	Mean broadleaf segment size (ha)
Site 1	87	58	6.06	27	8.33	31	4.25
Site 2	149	104	6.32	92	5.99	12	6.38
Site 3	72	39	3.02	34	3.06	5	3.69
Site 4	118	90	4.28	60	4.52	30	3.74
Total	426	291	4.90	220	5.14	71	4.18

Table 3. Crown sizes, by stand type.

	Mean (m^2)	Standard deviation (m^2)
All forested segments	8.2	1.3
Coniferous segments	7.8	1.0
Broadleaf segments	9.2	1.6

Table 4. Mean and standard deviation of image grey level values and tree crowns for segment-level metrics used as inputs to the regression tree.

	QuickBird grey-level values	
Metric	**Mean**	**Standard Deviation**
stand type (coniferous or broadleaf)	-	-
minority	152	148
majority	210	56
median	239	36
mean	245	34
standard deviation	69	16
range	480	116
variety	433	93
	Individual ITC-defined tree crowns	
crown closure (%)	46.0	6.6
mean crown size (m^2)	8.2	1.3
25^{th} percentile of crown size distribution (m^2)	3.7	0.5
50^{th} percentile of crown size distribution (m^2)	6.2	0.9
75^{th} percentile of crown size distribution (m^2)	10.5	1.7

Table 5. RMSE and R^2 for regression trees that included all of the metrics, or only an optimal set of metrics (for varying sizes of calibration data).

		Calibration sample size (%)									
		10	**20**	**30**	**40**	**50**	**60**	**70**	**80**	**90**	**100**
All metrics	R^2	NA	0.53**	0.50**	0.49**	0.49*	0.46	0.44*	0.44	0.45	0.26
	RMSE	NA	2.84	2.71	2.68	2.62	2.65	2.66	2.63	2.59	3.10
Optimal metrics only	R^2	NA	0.41**	0.38**	0.34**	0.31**	0.30**	0.29**	0.30**	0.31**	0.24**
	RMSE	NA	2.92	2.96	2.94	2.92	2.91	2.95	2.93	2.90	3.13

* $p < 0.05$; ** $p < 0.01$

Table 6. Welch test *p*-values indicating no significant difference between the manually interpreted and modeled mean stand heights for varying sizes of calibration data (α = 0.05).

	Calibration sample size (%)									
	10	**20**	**30**	**40**	**50**	**60**	**70**	**80**	**90**	**100**
All metrics	NA	0.75	0.86	0.79	0.69	0.83	0.70	0.79	0.79	0.80
Optimal metrics only	NA	0.52	0.49	0.40	0.52	0.57	0.52	0.55	0.53	0.56

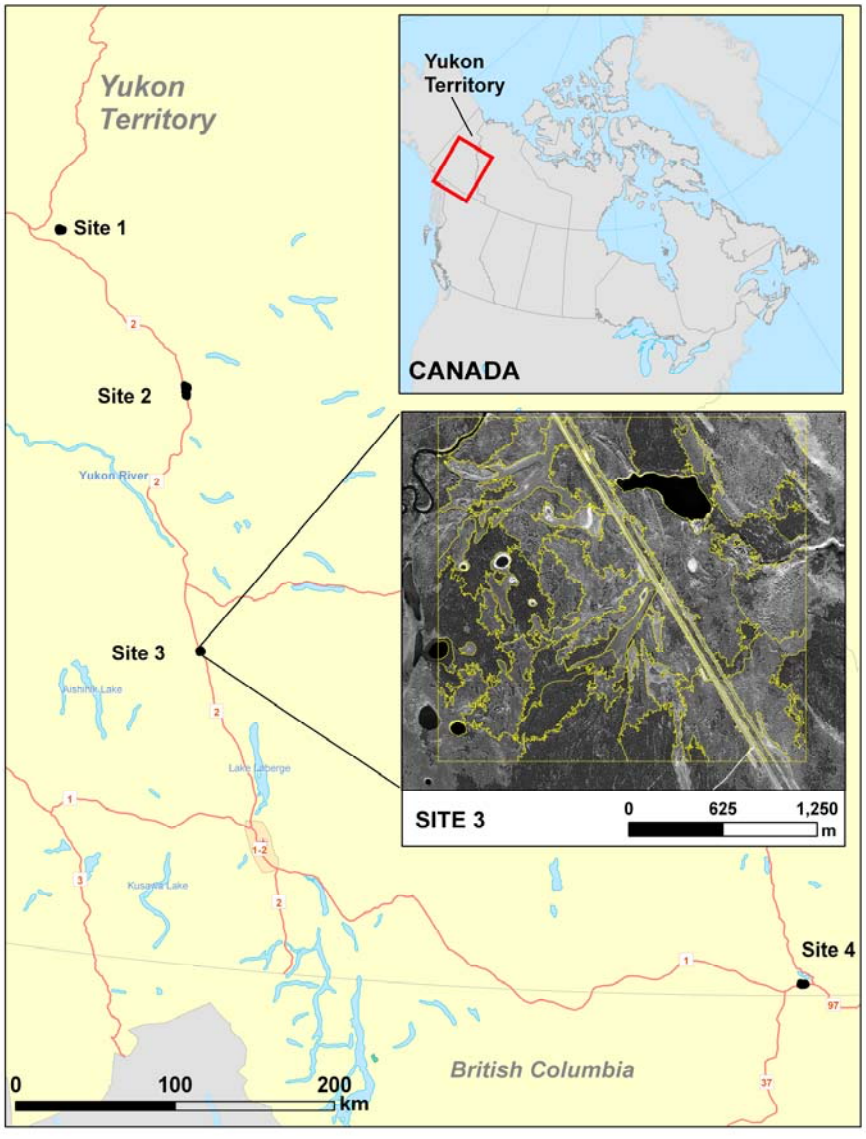

Figure 1. Study area located in the Yukon Terretory, Canada. The QuickBird image locations are also noted.

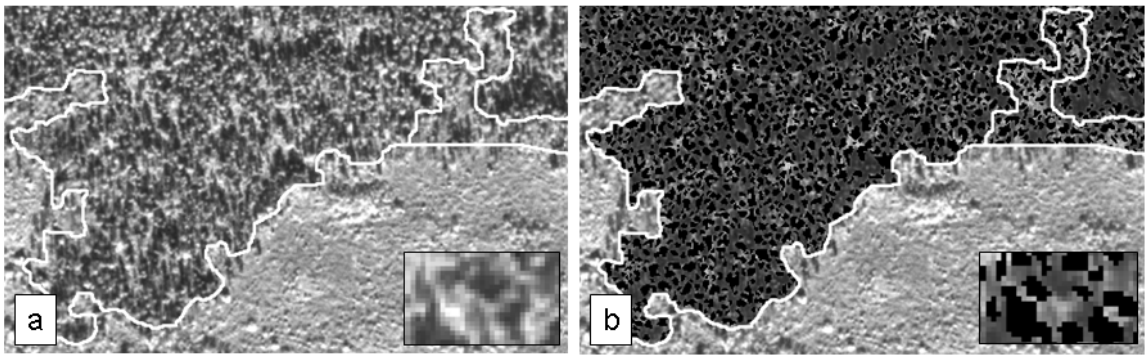

Figure 2: a) Stand delineation (white lines) with QuickBird imagery in background, b) Individual tree crown delineation using the ITC suite, with tree crown objects indicated in black. Within each inset is a focus graphic to show the QuickBird panchromatic imagery and resultant tree crowns.

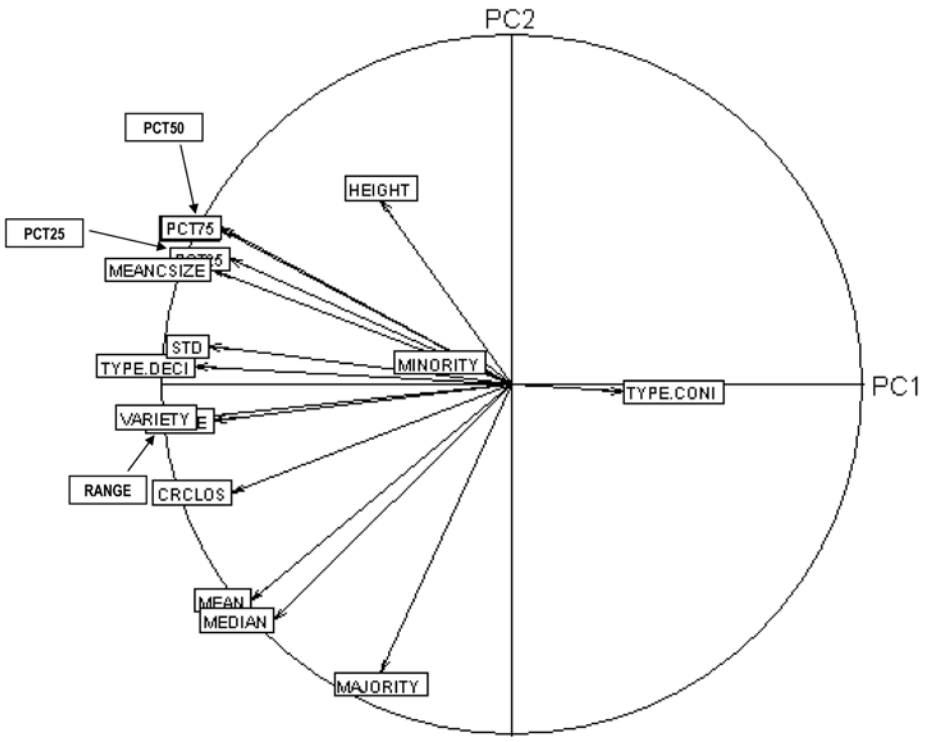

Figure 3. Correlation circle displaying the results of the Hill-Smith test applied to all the stand-level metrics (Table 2) versus the manually interpreted heights.

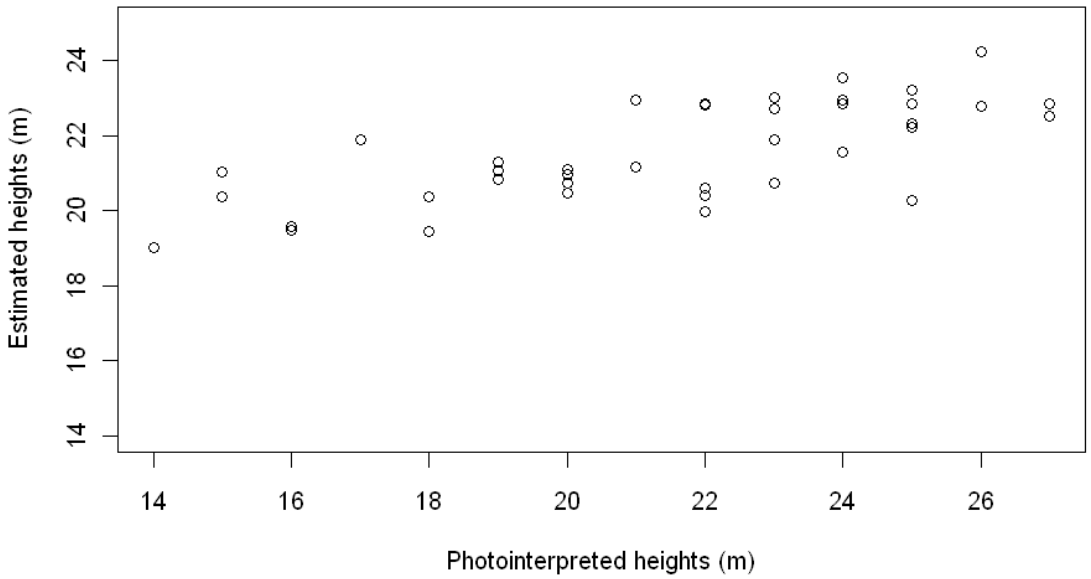

Figure 4. Plot of the manually interpreted heights versus estimated heights for the 30% calibration sample size.

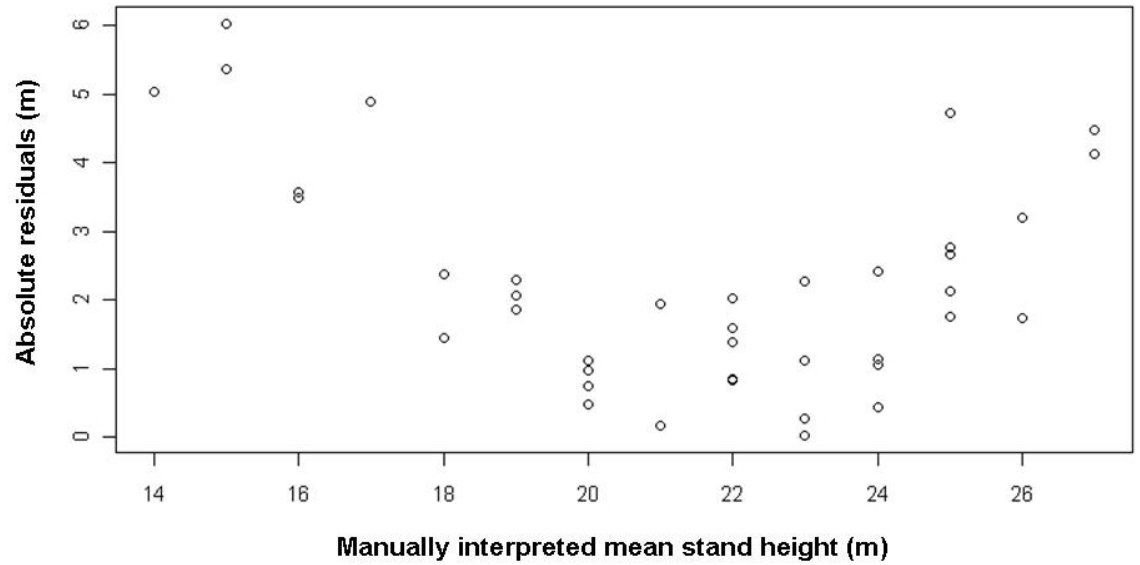

Figure 5. Plot of the absolute residual values versus the photo interpreted heights for the calibration sample size.

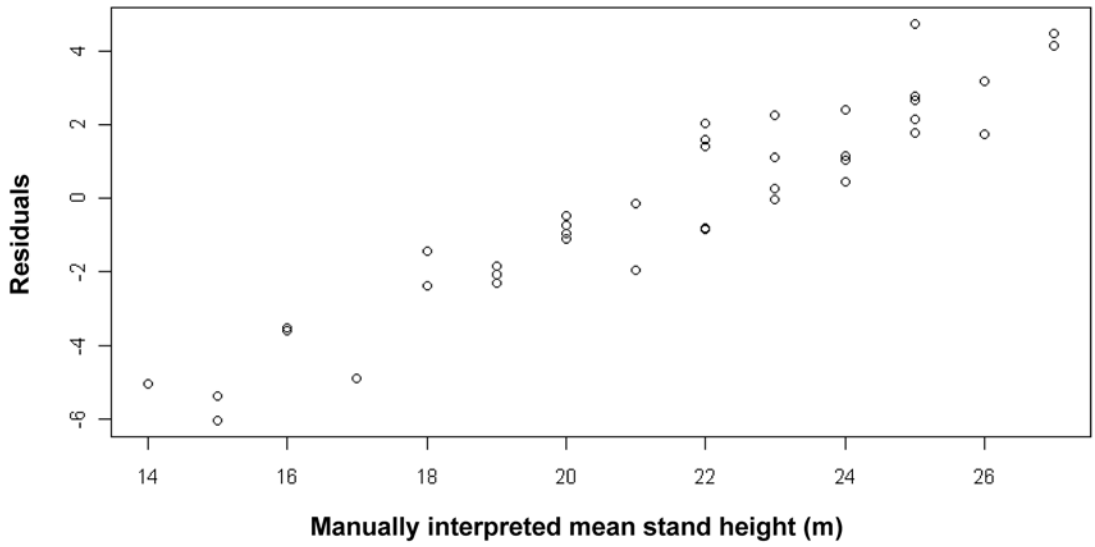

Figure 6. Plot of the residuals versus the photo interpreted heights for the 30% calibration sample size.